

Simultaneous Localization of Multiple Jammers and Receivers Using Probability Hypothesis Density

Sriramya Bhamidipati, *Student Member, IEEE* and Grace Xingxin Gao, *Senior Member, IEEE*

Abstract—Now-a-days, the availability of low-cost jammers in the commercial market is increasing. Due to this, there has been a rising risk of multiple jammers, not just one. However, it is challenging to locate multiple jammers because the traditional way of jammer localization via multilateration only works for one jammer. In addition, during attack the positioning capability of the receivers is compromised due to their inability to track the GPS signals.

We propose our Simultaneous Localization of Multiple Jammers and Receivers (SLMR) algorithm by utilizing the signal power received at a network of receivers. Our algorithm not only locates multiple jammers, but also utilizes the jammers as additional navigation signals for positioning the receivers. In particular, we design a non-linear Gaussian Mixture Probability Hypothesis Density Filter over a graphical framework, which is optimized using Levenberg-Marquardt minimizer. Under the presence of multiple simulated jammers, we validate that our proposed SLMR algorithm is able to simultaneously locate multiple jammers and receivers, even though the number of jammers is unknown.

I. INTRODUCTION

Due to the low signal power, GPS signals are vulnerable to external jamming attacks [1]-[2]. A jammer broadcasts high powered signals in the GPS frequency band [3] and causes the receiver to lose track of the satellite signals. This causes the Position Velocity and Time (PVT) solution to become unavailable for navigation.

Now-a-days, low-cost jammers are easily available in the commercial market [4]. Due to this, there is an increasing risk of imminent threats from multiple jammers, not just one [5]. Therefore, it is critical to account for the presence of multiple jammers to ensure prompt neutralization of all these malicious devices. In addition, given the inability of the receivers to track the GPS signals during jamming, we need alternate techniques to localize their position and facilitate robust continued operation.

The presence of multiple jammers gives rise to additional challenges because the traditional way of jammer localization via multilateration only works for one jammer. In addition, the number of jammers in the vicinity and their individual effect on the receiver is unknown. We propose our Simultaneous Localization of Multiple Jammers and Receivers (SLMR) algorithm to address the above-mentioned challenges due to multiple jammers. Our contributions are listed as follows

- 1) We utilize the front-end received power of GPS receivers to develop a robust algorithm which not only

estimates the number of jammers but also accurately locates them.

- 2) We also utilize the jammers as additional navigation signals to constrain the errors in the positioning of these network of receivers.
- 3) We develop a graphical framework constrained by the motion model and non-linear Gaussian Mixture Probability Hypothesis Density (GM-PHD) Filter [6]. We optimize the graph [7] to simultaneously locate the multiple jammers and receivers.

The rest of the paper is organized as follows: Section II describes our SLMR algorithm and its key characteristics; Section III experimentally validates the accuracy of our algorithm in locating the jammers and receivers by considering a network of receivers subjected to multiple simulated jammers; Section V concludes the paper.

II. SIMULTANEOUS LOCALIZATION OF MULTIPLE JAMMERS AND RECEIVERS (SLMR)

In this section, we describe the details of our proposed SLMR architecture, algorithm and the corresponding initialization requirements.

A. Our SLMR Architecture

We outline the steps in our SLMR architecture seen in Fig. 1 as follows

- 1) After jamming is detected using existing techniques [8]-[9], we initialize our SLMR algorithm and obtain the received power at all the L receivers.
- 2) We execute the update step of our non-linear GM-PHD Filter to compute the posterior intensity i.e., first order statistical moment of the relative state for each jammer-receiver pair. Based on this, we estimate the number of jammers M_t and the relative distances between jammers-receivers S_t .
- 3) Later, we optimize our sub-graph using LM algorithm to locate all the receivers $\vec{x}_{1:L,t}$ and the jammers $\vec{y}_{1:M_t,t}$ at the current time instant based on the constraints obtained from the update step of GM-PHD Filter, the receiver motion model and the last estimated position of receivers before being jammed.
- 4) We predict the posterior intensity for the next time instant after which the above steps are iterated over time to converge to the accurate number of jammers and

the locations of these multiple jammers and network of receivers. In addition, we also periodically execute full-graph optimization across all the time instants to further reduce the localization errors.

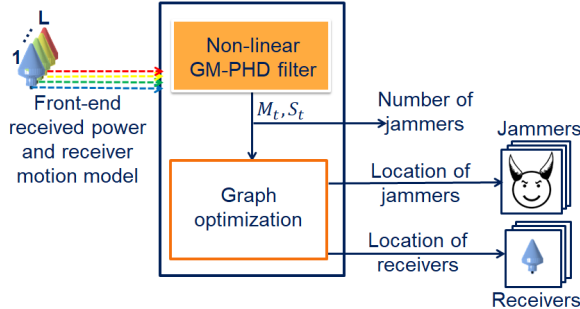


Fig. 1: Our SLMR architecture based on GM-PHD Filter and graph optimization to locate multiple jammers and receivers.

B. Our Algorithm

We describe our SLMR algorithm step-wise and also explain the corresponding theoretical formulation in detail.

1) Extract received power residuals:

For each i^{th} receiver, we compute the front-end received power a_i across the τ sample times over a period of ΔT time interval. Thereafter, we calculate the change in the received power denoted by z_i as

$$z_{i,t} = a_i - a_{i,int} = G_t G_r P_t \left(\frac{\lambda}{4\pi} \right)^2 \sum_k \left(\frac{1}{\eta_{ik}^2} \right) = \sum_k h_k(\eta_{ik,t}) \quad (1)$$

where $a_{i,int}$ represents the received power at the i^{th} receiver in authentic conditions computed during initialization, before the jamming attack is detected. $h_k(\cdot)$ denotes the measurement model based on free space path loss model [10], G_r and G_t represents the receiver and jammer antenna gain, P_t denotes the transmit power of the jammer and λ is the wavelength of the jamming signal, η_{ik} represents the relative distance vector between the i^{th} receiver and k^{th} jammer pair. $Z_i = \{z_i \in (1, \dots, L)\}$ represents the measurement vector given to the update step of our non-linear GM-PHD filter.

2) Formulate the graphical framework:

Considering the jammers and the motion of receivers to be independent of each other, in this step, we formulate a graphical framework to simultaneously localize the jammers and receivers in a sequential manner. For each i^{th} receiver, we design the graph seen in Fig. 2 as follows:

- 1) The blue nodes in the primary layer depict the sequential time series of its position and velocity $\bar{\mathbf{x}}_{i,1:t}$. The bottom layer of orange nodes represent the sequentially varying position and velocity of jammers $\bar{\mathbf{y}}_{1:M_t,1:t}$.
- 2) The top layer of orange nodes denoted by $u_{i,1:t}$ represent the sequential measurements obtained from the motion model of the i^{th} receiver.

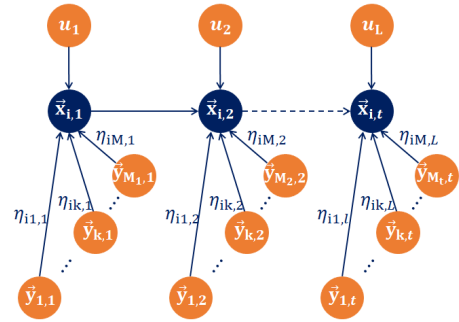


Fig. 2: Graphical framework for the i^{th} receiver. The orange nodes correspond to the motion model $u_{i,t}$ and the jammer navigation solution $\bar{\mathbf{y}}_{1:M_t,t}$. Blue nodes represent the sequential navigation solution $\bar{\mathbf{x}}_{i,1:t}$ of the i^{th} receiver.

In this layer as seen in Fig. 3, the unknowns are the position and velocity of the i^{th} receiver $\bar{\mathbf{x}}_{i,t} = [x, y, z, \dot{x}, \dot{y}, \dot{z}]_{i,t}^T$ and jammers $\bar{\mathbf{y}}_{1:M_t,t}$ at the current t^{th} time stamp which is computed using sub-graph optimization. The edges connecting the blue nodes to the orange nodes in bottom layer represent the constraint η_{ik} obtained from the update step of our GM-PHD Filter.

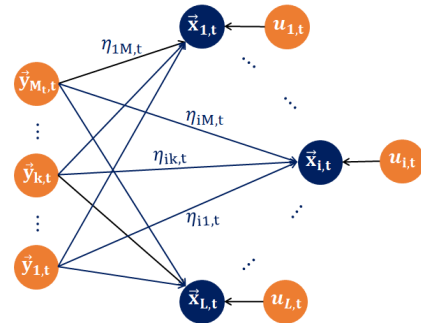


Fig. 3: Sub-graph at t^{th} time instant interconnecting different receivers via receiver motion model and received power.

3) Update step of non-linear GM-PHD Filter:

Due to the presence of multiple jammers, the probability distribution is multi-modal as seen in Fig. 4. In such conditions, implementing conventional bayes tracking [11] becomes computationally expensive. Therefore, in PHD Filter [12], we model our states as a Random Finite Set which represents the relative distance between each jammer-receiver pair and its cardinal number as a random variable which gives an estimate of the number of jammers.

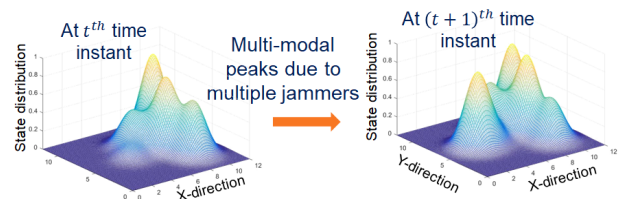


Fig. 4: Multi-modal distribution observed due to the presence of multiple jammers.

In our work, we formulate a non-linear formulation of GM-PHD Filter [6] where the multi-modal distribution is modeled as a Gaussian Mixture, to estimate the number of jammers M_t as well as the data association S_t among the L receivers and the predicted jammers.

The state vector S_t representing the relative distances between each jammer-receiver pair is defined as

$$S_t = \left\{ \eta_{ik,t}, i \in \{1, \dots, L\}, k \in \{1, \dots, M_t\} \right\} \quad (2)$$

First, we model the posterior intensity $\nu_t(\eta)$ as a Gaussian Mixture represented by

$$\nu_t(\eta) = \sum_{j=1}^{J_t} w_t^j \mathcal{N}(\eta; m_{t|t}^j, P_{t|t}^j) \quad (3)$$

Later, we compute the measurement update of the posterior intensity for each of the states $\eta \in S_t$ by dropping the subscript as

$$\begin{aligned} \nu_t(\eta) &= (1 - p_{D,t})\nu_{t|t-1}(\eta) + \sum_{z \in Z_t} \nu_{D,t}(\eta; z) \\ \nu_{D,t}(\eta; z) &= \sum_{j=1}^{J_{t|t-1}} w_t^j(z) \mathcal{N}(\eta; m_{t|t}^j(z), P_{t|t}^j) \\ w_t^j(z) &= \frac{p_{D,t} w_{t|t-1}^j q_t^j(z)}{\kappa_t(z) + p_{D,t} \sum_{l=1}^{J_{t|t-1}} w_{t|t-1}^l q_t^l(z)} \\ q_t^j(z) &= \mathcal{N}(z; H_k m_{t|t-1}^j, R_t + H_t P_{t|t-1}^j H_t^T) \\ m_{t|t}^j(z) &= m_{t|t-1}^j + K_t^j (z - H_t m_{t|t-1}^j) \\ P_{t|t}^j &= (I - K_t^j H_t) P_{t|t-1}^j \\ K_t^j &= P_{t|t-1}^j H_t^T (H_t P_{t|t-1}^j H_t^T + R_t)^{-1} \\ H_t &= \left. \frac{\partial h_k(\eta)}{\partial \eta} \right|_{\eta_t = m_{t|t-1}^j} \end{aligned} \quad (4)$$

where $\mathcal{N}(\cdot; m, P)$ denotes a Gaussian density with mean m and covariance P , H_t denotes the linearized measurement model, R_t is the measurement noise covariance and $p_{D,t}$ is a constant which denotes the detection probability. In the updated posterior intensity equations as seen in Eq. (4), $\nu_{D,t}(\eta; z)$ denotes the detection term for each $z \in Z_t$ while $(1 - p_{D,t})\nu_{t|t-1}(\eta)$ represents the mis-detection term corresponding to the state η . In addition, $w_t^j(z)$ denotes the detection weights allocated to each Gaussian density corresponding to each measurement of Z_k and $J_{t|t-1}$ indicates the total number of Gaussian densities predicted at the current t^{th} time instant. $m_{t|t-1}^j$ and $m_{t|t}^j$ denotes the predicted and updated mean of j^{th} Gaussian density. Similarly, $P_{t|t-1}^j$ and $P_{t|t}^j$ denotes the predicted and updated covariance of the j^{th} Gaussian distribution.

By executing this, the total number of Gaussian components increase from $J_{t|t-1}$ to $J_t = (L + 1) J_{t|t-1}$. We observe that the number of components increase without bounds thereby increasing the computational complexity.

Therefore, we next implement a pruning procedure to select the Gaussian components to be propagated to the next time.

We prune the Gaussian components based on their weights and the upper bound for the acceptable number of Gaussian components J_{max} . After the update step of our non-linear GM-PHD filter, we compute the state vector S_t of the current time instant t which equals the means of the Gaussian components $m_{t|t}^j$ with weights greater than a threshold T . The states of this estimated vector represent the relative distance between i^{th} receiver and k^{th} jammer. Based on this, the number of jammers are calculated as

$$M_t = (1 - p_{D,t}) M_{t|t-1} + \frac{1}{L} \sum_{j=1}^{J_{t|t-1}} w_t^j(z) \quad (5)$$

$$S_t = \left\{ m_{t|t}^j, j \in \{1, \dots, J_t\} \mid m_{t|t}^j > T \right\}$$

4) Optimize the sub-graph and full-graph:

In this step, we optimize the sub-graph seen in Fig. 3, using the objective function \mathbf{F}_t which consists of three components [13].

$$\begin{aligned} \mathbf{F}_t(\mathbf{x}_{1:L,t}, \mathbf{y}_{1:M_t,t}) &= \sum_i \mathbf{x}_{i,int}^T \Omega_{i,int} \mathbf{x}_{i,int} + \\ &\sum_i \sum_k \left(\eta_{ik,t} - h_k(\mathbf{x}_{i,t}, \mathbf{y}_{k,t}) \right)^T \Sigma_t^{-1} \left(\eta_{ik,t} - h_k(\mathbf{x}_{i,t}, \mathbf{y}_{k,t}) \right) \\ &+ \sum_i \left(\mathbf{x}_{i,t} - g(u_t, \mathbf{x}_{i,t-1}) \right)^T \Omega_{i,t}^{-1} \left(\mathbf{x}_{i,t} - g(u_t, \mathbf{x}_{i,t-1}) \right) \end{aligned} \quad (6)$$

where Σ_t denotes the associated covariance involved. $\Omega_{i,int}$, $\Omega_{i,t}^{-1}$ denote the covariances of the position of the i^{th} receiver during initialization and at the t^{th} time instant respectively.

Firstly, the initial constraint $\mathbf{x}_{1:L,int}$, which corresponds to the L receivers, marks the global reference point for the estimation of receiver and jammer locations. In the second component, we compare the constraints M_t and S_t obtained from the update step of our non-linear GM-PHD Filter to that of the expected measurement model $h_k(\cdot)$ summed across each jammer-receiver pair. Lastly, we compare the unknown position and velocity of the receiver to be estimated with that of the expected position of receiver based on motion model $g(\cdot)$. The motion model is obtained from either the vehicle dynamics or external sensors. Thereafter, we carry out the optimization procedure using a LM minimizer to estimate the variables $(\mathbf{x}_{1:L,t}, \mathbf{y}_{1:M_t,t})$.

After this, we correct the state vector S_t based on the sub-graph estimates of the receivers $\mathbf{x}_{1:L,t}$ and jammers $\mathbf{y}_{1:M_t,t}$ which is given as input to the prediction step of our non-linear GM-PHD Filter.

Based on the current estimate of the number of jammers M_t , we periodically execute full-graph optimization across time to constrain the drifts and to reduce the localization errors in the estimates of $(\mathbf{x}_{1:L,t}, \mathbf{y}_{1:M_t,t})$. This is executed by minimizing the objective function given by

$$(\mathbf{x}_{1:L,1:t}, \mathbf{y}_{1:M_t,1:t}) = \operatorname{argmin}_t \mathbf{F}_t(\mathbf{x}_{1:L,t}, \mathbf{y}_{1:M_t,t}) \quad (7)$$

5) Predict step of non-linear GM-PHD Filter:

We compute the predicted intensity for the next instant $t + 1$ as follows

$$\begin{aligned}
 \nu_{t+1|t}(\eta) &= \nu_{S,t+1|t}(\eta) + \gamma_{t+1}(\eta) \\
 \nu_{S,t+1|t}(\eta) &= p_{S,t} \sum_{j=1}^{J_t} w_t^j \mathcal{N}(\eta; m_{S,t+1|t}^j(z), P_{S,t+1|t}^j) \\
 \gamma_{t+1}(\eta) &= \sum_{j=1}^{J_{\gamma,t+1}} w_{\gamma,t+1}^j \mathcal{N}(\eta; m_{\gamma,t+1}^j(z), P_{\gamma,t+1}^j) \\
 M_{t+1|t} &= p_{S,t} M_t + \frac{1}{L} \sum_{j=1}^{J_{\gamma,t}} w_{\gamma,t}^j \\
 m_{S,t+1|t}^j &= F_t m_t^j \\
 P_{S,t+1|t}^j &= Q_t + F_t P_t^j F_t^T
 \end{aligned} \tag{8}$$

where p_S is considered a constant which denotes the survival probability, F_t is obtained from the motion model $g(\cdot)$, Q_t denotes the process noise covariance, $\nu_{S,t+1}(\eta; z)$ denotes the survival term and $m_{S,t+1|t}^j, P_{S,t+1|t}^j$ denotes the mean and covariance of the survival categorized Gaussian components. $\gamma_{t+1}(\eta)$ denotes the birth intensity of a jammer. The corresponding birth parameters are denoted by weights $w_{\gamma,t+1}$, mean $m_{\gamma,t+1}^j$, covariance $P_{\gamma,t+1}$ and number of birth Gaussian Mixture $J_{\gamma,t+1}$. $M_{t+1|t}$ denotes the predicted number of states in our GM-PHD Filter. Thereafter, the entire process repeats itself to converge over time.

C. Initialization

After the jamming is detected, we initialize our algorithm in three parts: Firstly for each receiver, we compute the average of the most recent V measurements in non-jammed, authentic conditions to compute $a_{i,int} = \frac{1}{V} \sum_v (a_{i,-v})$, $i \in \{1, \dots, L\}$. In addition, we also extract the position and velocity of all the L receivers and their corresponding covariance involved i.e., $\bar{x}_{1:L,int}, \Omega_{1:L,int}$.

Secondly, we initialize our non-linear GM-PHD Filter and the sub-graph, by considering a single jammer to be present at the centroid of the known receivers' position and velocity denoted by $\bar{x}_{1:L,int}$.

III. EXPERIMENTAL RESULTS

In this section, we demonstrate the simulated experimental results to validate our SLMR algorithm by considering a network of receivers. We consider a network of widely dispersed five vehicles each equipped with a GPS receiver. The dynamics of the vehicles and their corresponding receiver errors are considered independent of each other. The trajectories followed by each of the vehicles is shown in the Fig. 5. We considered three stationary jammers shown by black dots in Fig. 5 transmitting simulated sweep jamming attack with transmission power of $50.3 W$ based on free space path loss model.

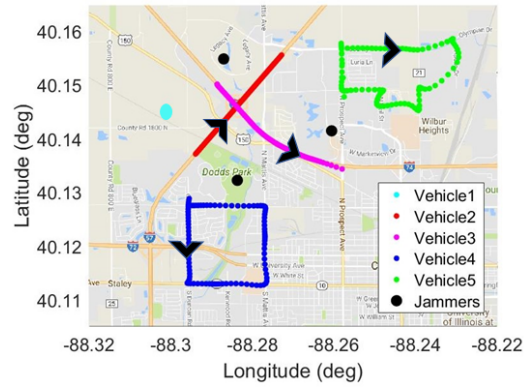


Fig. 5: Our experimental setup consists of five vehicles each equipped with a GPS receiver. The vehicle trajectories are indicated by cyan, red, magenta, blue and green. The location of three jammers considered are shown in black.

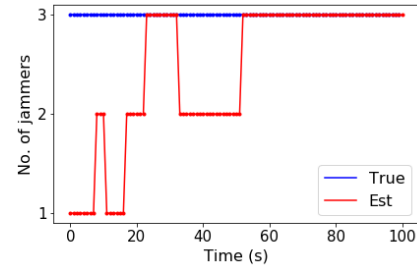


Fig. 6: Under simulated sweep continuous jamming attack: Number of jammers estimated using our algorithm are shown by the red dots and the actual number of jammers are shown in blue. We observed that our algorithm accurately converges to the actual number of jammers present i.e., 3 in $\approx 60 s$.

Fig. 6 showed the estimated number of jammers indicated in red using our SLMR algorithm whereas the blue indicate the actual number of jammers present i.e., 3. We observed that our algorithm efficiently utilized the receiver motion model and their corresponding received power measurements to accurately estimate the jammers in $\approx 60 s$.

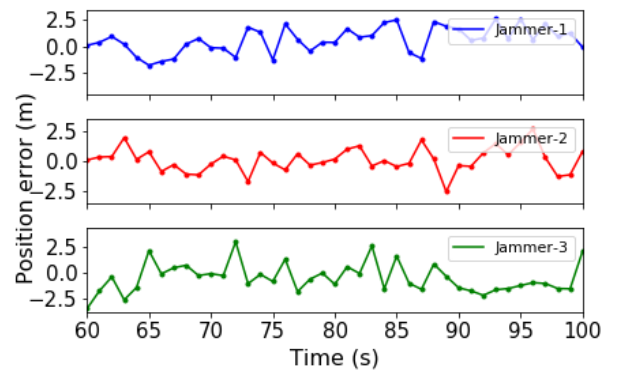


Fig. 7: Position error of multiple jammers. We showed that our algorithm accurately estimated the locations of multiple jammers to within $5 m$ accuracy.

Next, we estimated the total error in the location of multiple jammers, obtained as output from sub-graph optimization, after our algorithm has converged. In Fig. 7 and Fig. 8, we demonstrated that our proposed SLMR algorithm accurately estimated the location of jammers to within $5 m$ and receivers to within $7.3 m$ accuracy.

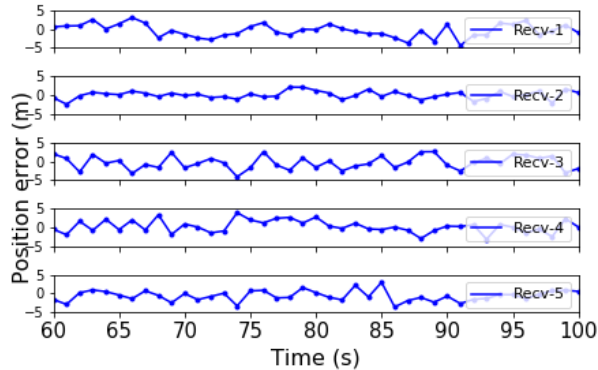


Fig. 8: Position error of receivers. We showed that our algorithm accurately estimated the locations of the network of receivers to within $7.3 m$ accuracy.

IV. CONCLUSIONS

We proposed our SLMR algorithm that not only is able to locate multiple jammers, but also the receivers by utilizing the received jamming signals as additional information sources. We achieved this by designing a robust graphical framework constrained using GM-PHD Filter and optimized using LM algorithm. Under the presence of multiple simulated jammers, our results validated the accuracy of our SLMR algorithm in estimating the actual number of jammers and computing the position of jammers and receivers to within $5 m$ and $7.3 m$ accuracy.

ACKNOWLEDGMENT

This material is based upon work supported by the Department of Energy under Award Number DE-OE0000780.

This report was prepared as an account of work sponsored by an agency of the United States Government. Neither the United States Government nor any agency thereof, nor any of their employees, makes any warranty, express or implied, or assumes any legal liability or responsibility for the accuracy, completeness, or usefulness of any information, apparatus, product, or process disclosed, or represents that its use would not infringe privately owned rights. Reference herein to any specific commercial product, process, or service by trade name, trademark, manufacturer, or otherwise does not necessarily constitute or imply its endorsement, recommendation, or favoring by the United States Government or any agency thereof. The views and opinions of authors expressed herein do not necessarily state or reflect those of the United States Government or any agency thereof.

REFERENCES

- [1] S. Pullen, G. X. Gao, C. Tedeschi, and J. Warburton, "The impact of uninformed RF interference on GBAS and potential mitigations," In Proceedings of the 2012 International Technical Meeting of the Institute of Navigation (ION ITM 2012), Newport Beach, CA, Jan. 2012, pp.780789.
- [2] F. Dovis ed., "GNSS Interference Threats and Countermeasures," Artech House; 2015 Feb 1.
- [3] R. H. Mitch, M. L. Psiaki, B. W. O'Hanlon, S. P. Powell, J. A. Bhatti, "Civilian GPS jammer signal tracking and geolocation," In ION GNSS 2012 Sep 18.
- [4] G. X. Gao, M. Sgammini, M. Lu, N. Kubo, "Protecting GNSS receivers from jamming and interference," In Proceedings of the IEEE. 2016 Jun;104(6):1327-38.
- [5] S. Rounds, "Innovation-Jamming Protection of GPS Receivers-Part II: Antenna Enhancements-The second article in a two-part series about jamming protection for GPS receivers looks at enhancements to antenna," GPS World. 2004;15(2):38-45.
- [6] B. N. Vo, W. K. Ma, "The Gaussian mixture probability hypothesis density filter," In IEEE Transactions on signal processing. 2006 Nov;54(11):4091-104.
- [7] J. J. Mor, "The Levenberg-Marquardt algorithm: implementation and theory," In Numerical analysis 1978 (pp. 105-116). Springer, Berlin, Heidelberg.
- [8] K. G. Gromov, D. Akos, S. Pullen, P. Enge, B. Parkinson, "GIDL: Generalized interference detection and localization system," In 10th Saint Petersburg International Conference on Integrated Navigation Systems 2002 Mar.
- [9] K. A. Shridhara, "Jamming detection and blanking for GPS receivers," United States patent US 6,448,925. 2002 Sep 10.
- [10] V. Erceg, L. J. Greenstein, S. Y. Tjandra, S. R. Parkoff, A. Gupta, B. Kulic, A. A. Julius, R. Bianchi, "An empirically based path loss model for wireless channels in suburban environments," IEEE Journal on selected areas in communications. 1999 Jul;17(7):1205-11.
- [11] Y. Bar-Shalom, X. R. Li, "Multitarget-multisensor tracking: principles and techniques," London, UK.: YBs; 1995 Sep.
- [12] K. Panta, B. N. Vo, S. Singh, "Novel data association schemes for the probability hypothesis density filter," IEEE Transactions on Aerospace and Electronic Systems. 2007 Apr;43(2).
- [13] F. Schuster, C. G. Keller, M. Rapp, M. Haueis, C. Curio, "Landmark based radar slam using graph optimization," In Intelligent Transportation Systems (ITSC), 2016 IEEE 19th International Conference on 2016 Nov 1 (pp. 2559-2564). IEEE.

BIOGRAPHIES

Sriramya Bhamidipati is a doctoral student in the Aerospace Engineering Department at the University of Illinois at Urbana-Champaign. She received her M.S degree in Aerospace Engineering from University of Illinois at Urbana-Champaign in 2017. She received her B.Tech. with honors in Aerospace Engineering and minor in Systems and Controls Engineering from Indian Institute of Technology Bombay, India in 2015.

Grace Xingxin Gao received the B.S. degree in Mechanical Engineering and the M.S. degree in electrical engineering from Tsinghua University, Beijing, China in 2001 and 2003. She received the PhD degree in Electrical Engineering from Stanford University in 2008. From 2008 to 2012, she was a research associate at Stanford University. Since 2012, she has been with University of Illinois at Urbana-Champaign, where she is presently an assistant professor in the Aerospace Engineering Department.